Conformational Study of Silk-Like Peptides Containing the Calcium-Binding Sequence from Calbindin D_{9k} Using ^{13}C CP/MAS NMR Spectroscopy

Tetsuo Asakura,*,† Megumi Hamada,† Yasumoto Nakazawa,† Sung-Won Ha,† and David P. Knight‡

Department of Biotechnology and Life Science, Tokyo University of Agriculture and Technology, Koganei, Tokyo 184-8588, Japan, and Department of Zoology, University of Oxford, South Parks Roads, Oxford OX1 3PS, United Kingdom

Received November 13, 2005; Revised Manuscript Received December 12, 2005

The calcium-binding sites of calbindin D_{9k} have a helix−loop−helix motif. In this study, the helix motifs were replaced by several Ala-Gly repeating regions designed on the basis of the primary sequences of several silk fibroins. The synthesized peptides were treated with several organic solvents to modify the secondary structure of the Ala-Gly repeating regions. The local structures of the Ala-Gly repeating regions, as well as the calcium-binding motif, D_{9k}-loop ($D_{9k}L$), were determined by ^{13}C CP/MAS NMR spectroscopy. In the four peptides containing $D_{9k}L$ synthesized, the poly(Ala) domains retain the ability to undergo a conformational transition from α-helical to β-sheet in $(A)_{12}$-$D_{9k}L$ despite the presence of the $D_{9k}L$ domain at the center of the peptide molecule, but the presence of this domain in the other model peptides synthesized has a marked effect on the conformation of the added silk-like domains. The results showed that the structures of the Ala-Gly repeating regions can be controlled by the choice of both the organic solvent and the amino acid sequence of the Ala-Gly repeating regions without disrupting the secondary structure of $D_{9k}L$ suggesting that it may retain its ability to bind calcium ions.

Introduction

Silks have long attracted attention as biodegradable and resorbable fibers with considerable strength, elasticity, and durability.[1] Silk fibers are produced from various types of ectodermal glands in mites, spiders, and several groups of insects.[2] Each of these different silks exhibits mechanical properties tailored to their specific functions. Silks are encoded by highly repetitive structural genes that are under tight regulatory control in the cell. Silks from different species have their own unique amino acid compositions and primary sequences (Figure 1). For instance, the repetitive primary sequences in *Bombyx mori* (*B. mori*) are dominated by iterations of a GAGAGS motif[3,4] while blocks of poly(Ala) separated by glycine-rich blocks make up the repetitive structure in *Antheraea pernyi* (*A. pernyi*) cocoon silk fibroin[5,6] and *Nephila clavipes* (*N. clavipes*) dragline silk spidroin.[7] These highly repetitive primary sequences lead to significant homogeneity in secondary structure, predominantly β-sheet for most silks. Highly ordered β-sheets oriented along the fiber axis contribute to the excellent mechanical properties of silks, which create an expectation that silks could be extremely useful as implantable biomaterials and scaffolds for tissue engineering. In addition, silk fibroins are capable of mineralization with hydroxyapatite.[8,9] Our study was further motivated by three lines of evidence suggesting that calcium ion binding may play a role in the natural spinning process in lepidopterans: 1. Calcium ions induce reversible gel formation in native *B. mori* silk fibroin.[10−12] 2. High concentrations of calcium ions play a role in stabilizing the silk I conformation, whereas low concentrations may promote the formation of silk II.[13] 3. The well conserved N-termini of lepidopteran fibroins are markedly acidic, containing high concentrations of glutamic acid residues[14] potentially capable of binding calcium ions, while LALIGN analysis[15] of the N-termini showed sequence similarity with the EF-hand calcium binding motifs in calmodulin and calbindin.[16] Accordingly, we aimed in the present study to produce synthetic silk-like peptides

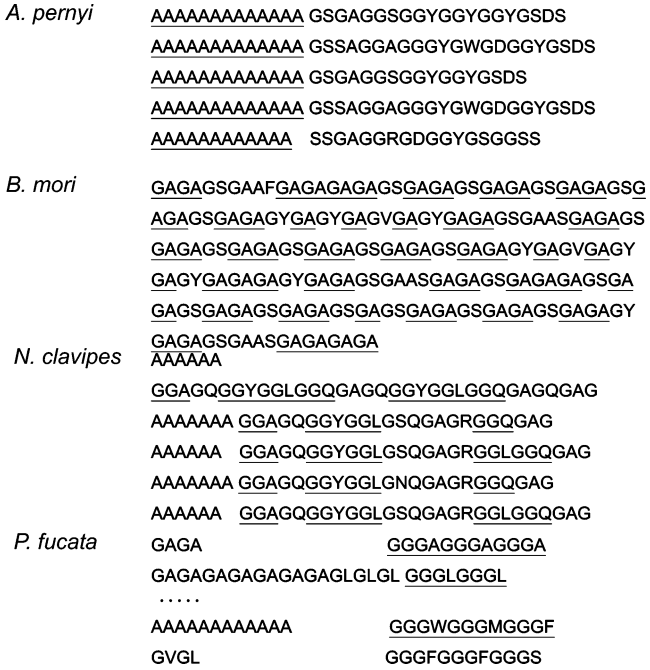

Figure 1. Amino acid sequences taken from *Antheraea pernyi* and *Bombyx mori* silk fibroin, *Nephila clavipes* dragline silk spidroin 1 (MaSp1), and *Pinctada fucata* insoluble protein. Characteristic repetitive motifs are underlined.

* To whom correspondence should be addressed. Tel&Fax: +81-42-383-7733. E-mail: asakura@cc.tuat.ac.jp.

† Tokyo University of Agriculture and Technology.

‡ University of Oxford.

10.1021/bm050863q CCC: $33.50
Published on Web 01/17/2006

Table 1. Amino Acid Sequences of Six Peptides Synthesized in This Study

sample name	amino acid sequence
D_{9k}-loop (D_{9k}L)	GAAKEGDPNQLSKEEG
$(A)_{12}$-D_{9k}L	AAAAAAAAAAAAAAKEGPNQLSKEEAAAAAAAAAAAA
$(AG)_6$-D_{9k}L	AGAGAGAGAGAGAAKEGDPNQLSKEEAGAGAGAGAGAG
$(AGG)_4$-D_{9k}L	AGGAGGAGGAGGAAKEGDPNQLSKEEAGGAGGAGGAGG
$(AGGG)_3$-D_{9k}L	AGGGAGGGAGGGAAKEGDPNQLSKEEAGGGAGGGAGGG
^{13}C-labeled $(A)_{12}$-D_{9k}L	AAAAAA[1-^{13}C]AAAAAA[2-^{13}C]A[3-^{13}C]AKE[2-^{13}C]GPNQLSKEEAAAAAAAAAAAA

containing the EF-hand calcium-binding motif of calbindin, the D_{9k}-loop (D_{9k}L).[17,18] The primary sequence of D_{9k}L was introduced into four different kinds of peptides each with a different repeating sequence of Ala and Gly found frequently in the primary structure of silk fibroins.

Calbindin D_{9k} is a small, acidic, and heat-stable protein found in the small intestine of all mammalian species.[17,18] It is reported that this protein may be involved in fetal calcium uptake, uterine contractions, calcification of bone and teeth, and calcium transport and uptake in mammalian intestine.[19] Calbindin D_{9k} binds Ca^{2+} with very high affinity ($K = 10^8$ M^{-1}). It belongs to the calmodulin superfamily of calcium-binding proteins characterized by the possession of a common helix-loop-helix motif for calcium-binding sites, termed the EF-hand.[20] The three-dimensional structure of bovine calbindin D_{9k} in the calcium-loaded state has been determined by X-ray crystallography.[21] The solution structures of both calcium-loaded and unloaded calbindin D_{9k} have also been determined by NMR spectroscopy.[22,23]

Here, we synthesized four different types of peptides containing ^{13}C labeled Ala and Gly and the EF-hand calcium-binding motif. We obtained secondary structural information for these peptides using ^{13}C CP/MAS NMR spectroscopy. The structure of the Ala-Gly repeating regions of the peptides was compared to that of other synthetic peptides each with the same primary sequence except with the omission of the D_{9k}L EF-hand motif. The isotopic ^{13}C chemical shifts of the C_α, C_β, and carbonyl carbons (C═O) provide selective and detailed conformational information without interfering with the folding of the peptides. The detailed structural analyses of these peptides should provide useful information toward the development of silk-based biomaterials containing a high affinity calcium-binding motif.

Materials and Methods

Sample Preparations. The following peptides D_{9k}-loop (D_{9k}L); $(A)_{12}$-D_{9k}L; $(AG)_6$-D_{9k}L; $(AGG)_4$-D_{9k}L; $(AGGG)_3$-D_{9k}L, and selectively ^{13}C isotope labeled $(A)_{12}$-D_{9k}L ([1-^{13}C]A7, [2-^{13}C]A13, [3-^{13}C]A14, [2-^{13}C]G17) were synthesized by the Fmoc solid-phase method (Table 1). After syntheses, samples were dissolved in 9 M lithium bromide (LiBr) and dialyzed (MWCO = 1,000 Da, Spectra/Por) against distilled water for 4 days at 4 °C. The naturally precipitated samples after dialysis were collected and freeze-dried. The freeze-dried peptides were treated either with trifluoroacetic acid (TFA), LiBr, or formic acid (FA) as follows: 1. dissolution in TFA followed by precipitation in diethyl ether (TFA treatment); 2. dissolution in FA followed by air-drying (FA treatment); 3. dissolution in 9 M LiBr followed by dialysis against 3 M LiBr aqueous solution (3 h), a final dialysis against distilled water (4 days) before air drying (LiBr treatment). The treatments are known to produce changes in secondary structure in silk-like peptides.[24−26]

^{13}C CP/MAS NMR Spectroscopy. The ^{13}C CP/MAS NMR experiments were performed at 25 °C with a CMX Infinity 400 NMR spectrometer (Chemagnetics) operated at 100.04 MHz for the ^{13}C nucleus. Each sample was placed in a cylindrical rotor and spun at a rate of 10 kHz. The number of acquisitions was 12 000, and the pulse delays were 3 s. For decoupling, 50 kHz radio frequency field strength was used with a decoupling period of 12.8 ms. A 90° pulse width of 3.2 μs with 1 ms CP contact time was employed. Phase cycling was used to minimize artifacts. ^{13}C chemical shifts were calibrated indirectly through the adamantane methyl peak observed at 28.8 ppm relative to tetramethylsilane at 0 ppm.

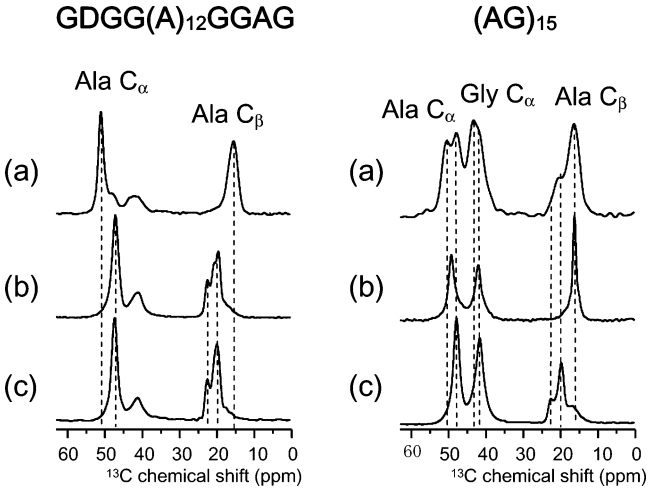

Figure 2. ^{13}C CP/MAS NMR spectra of Ala-Gly repeated model peptides, GGDG$(A)_{12}$GGAG and $(AG)_{15}$ after TFA treatment (a), LiBr treatment (b), and FA treatment (c). The peak assignments are included.

Results and Discussion

Secondary Structure of Four Silk-Like Peptides with Different Repeating Sequences of Ala and Gly after TFA, LiBr, and FA Treatments. Figure 2 shows ^{13}C CP/MAS NMR spectra (0∼60 ppm) of GDGG$(A)_{12}$GGAG (left) and $(AG)_{15}$ (right) after TFA, LiBr, and FA treatments. The ^{13}C chemical shifts of the corresponding carbon atoms of these peptides are listed in Table 2. The ^{13}C chemical shift values of Ala and Gly residues for proteins with typical conformation are also listed, where the random coil chemical shifts were obtained from the ^{13}C solution NMR.[27] In the latter paper, it was difficult to distinguish silk II from β-sheet because of peak overlap. We therefore used silk II for both $(AG)_{15}$ and $(AG)_{15}$-D_{9k}L, and β-sheet for other cases according to our previous reports.[28,29] The peptide, GDGG$(A)_{12}$GGAG, was synthesized previously as models to examine the structure of *S. c. ricini* silk fibroin before (TFA treatment) and after (FA treatment) fiber formation. The TFA treatment induces α-helix for the poly(Ala) region, whereas the FA treatment induces the β-sheet structure for the same region. This was concluded from the ^{13}C chemical shifts of the main peaks assigned to the C_α and C_β of alanine residues. The asymmetric spectral pattern of Ala C_β indicates additional heterogeneous β-sheet structure.[29,30] The contribution of additional GDGG and GGAG sequences (at the N- and C-terminus, respectively) to the conformation of the peptides has been discussed previously in detail.[24,31] The newly observed ^{13}C CP/MAS NMR spectrum of the peptide after dissolving it in 9 M LiBr and then dialyzing against water suggests that the peptide also takes heterogeneous β-sheet structure, which is similar to the structure of the peptide after FA treatment. However, the Ala C_β peak pattern is slightly different from the pattern after FA treatment: The chemical shift of the lowest

Table 2. ^{13}C Chemical Shifts (in ppm from TMS) of Eight Peptides Synthesized Here after TFA Treatment, LiBr Treatment, and FA Treatment[a]

		^{13}C chemical shifts (ppm)					
peptides	treatment	Ala C_α	Ala C_β	Ala C=O	Gly C_α	Gly C=O	conformation
GDGG$(A)_{12}$GGAG	TFA	52.5	15.7	176.2			α-helix
	LiBr	48.5	20.0, 21.3, 22.9	171.8			β-sheet
	FA	48.7	20.3,23.0	171.9			β-sheet
$(AG)_{15}$	TFA	48.7, 51.4	16.1, 20.0	176.4	44.6	169.4, 172.3	mixture of random coil and silk II
	LiBr	50.7	16.5	176.8	43.2	169.9	silk I
	FA	48.7	16.7, 19.6, 22.2	171.8	42.4	171.8	silk II
$(AGG)_{10}$	TFA	49.9	16.7	172.2	43.2	172.2	random coil
	LiBr	48.9	17.4	174.6	41.6	171.3	3_1-helix
	FA	48.8	17.3	174.6	41.4	171.2	3_1-helix
$(AGGG)_7$	TFA	49.0	16.5, 20.8	175.3	42.4	171.6	mixture of random coil and β-sheet
	LiBr	48.8	17.8, 21.1	173.9	42.5	168.1, 171.5	mixture of distorted 3_1-helix and β-sheet
	FA	48.9	16.8, 21.3	172.3	43.7	168.5	mixture of random coil and β-sheet
$(A)_{12}$-D_{9k}L	TFA	52.6	15.9	175.8			α-helix
	LiBr	48.1	19.5, 23.0	171.3			β-sheet
	FA	48.7	20.0, 23.1	171.9			β-sheet
$(AG)_6$-D_{9k}L	TFA	48.7	16.1, 20.8	172.1	42.2	168.9	mixture of random coil and silk II
	LiBr	50.0	16.4	-	42.8	-	random coil
	FA	48.9	17.9, 20.9	172.5	42.7	168.5	silk II
$(AGG)_4$-D_{9k}L	TFA	49	16.0	-	42.0	-	random coil
	LiBr	48.7	17.1	172.4	41.5	171.2	distorted 3_1-helix
	FA	48.5	16.4	-	41.4	-	random coil
$(AGGG)_3$-D_{9k}L	TFA	50	16.6	-	42.6	-	random coil
	LiBr	50	16.5	-	42.7	-	random coil
	FA	49.3	17.1	-	42.4	-	mixture of random coil and β-sheet
reference ^{13}C		50.0	16.6	175.5	42.7	171.3	random coil (from solution NMR)
chemical shift values of proteins with typical conformation		52.5	15.7	176.5	44.0	172.3	α-helix
		48.7	16.7, 19.6, 22.2	171.8	42.4	169.1	silk II (β-sheet)
		48.9	17.4	174.6	41.6	171.3	3_1-helix

[a] The chemical shifts for the amino acid residue with typical structure are also shown.

field peak assigned to β-sheet is the same, 23.0 ppm for both treatments, but the higher field peaks observed as single peak at 20.3 ppm after FA treatment becomes asymmetric (20.0 ppm main peak and 21.3 ppm shoulder peak) after LiBr treatment.

$(AG)_{15}$ has been considered as a model of the crystalline region, $(AGSGAG)_n$, of *B. mori* silk fibroin. Several ^{13}C and ^{15}N labeled $(AG)_{15}$ were synthesized for different types of solid-state NMR analyses.[25] After LiBr treatment, the structure of $(AG)_{15}$ takes a repeated β-turn type II structure making it a structural model for the conformation of this region before spinning. The sharp peak at 16.5 ppm observed for the Ala C_β is indicative of the proposed structure.[25,32] After FA treatment, the structure changes completely to silk II structure, the structure after spinning. The silk II structure was characterized by about 70% β-sheet structure with two different intermolecular arrangements and 30% distorted β-turn.[26,33] This was concluded using ^{13}C CP/MAS NMR spectra for detailed analysis of Ala C_β in both $(AG)_{15}$ and the C_p fraction (the crystalline portion after chymotrypsin cleavage of *B. mori* silk fibroin) and also the *B. mori* silk fibroin fiber. Thus, the structure of $(AG)_{15}$ is different after LiBr and FA treatments. This is completely different from the case of GDGG$(A)_{12}$GGAG mentioned above. The newly observed spectrum of $(AG)_{15}$ after TFA treatment indicates that both the random coil and the β-sheet structure coexists although the fraction of the former conformation is larger than after FA treatment. This is clear from the doublet peaks at both C_α and C_β of the Ala residue. The asymmetric Gly C_α peak also indicates the presence of both conformations.

$(AGG)_{10}$ takes a unique structure after both LiBr or FA treatments, the 3_1-helix as shown in Figure 3 (left).[22] The detailed characterization of the 3_1-helix has been performed previously using the 2-D spin diffusion NMR and REDOR techniques. The chemical shift, 17.3 ppm of Ala C_β is characteristic of the 3_1-helix. The Ala C_β peak is slightly broader for LiBr treatment compared with the width of the corresponding peak after FA treatment, indicating a relatively larger distribution of the torsion angles of the backbone chains. The newly observed spectrum of $(AGG)_{10}$ after TFA treatment becomes broader and the chemical shifts of Ala and Gly carbons shift to typical values of random coil chemical shifts.

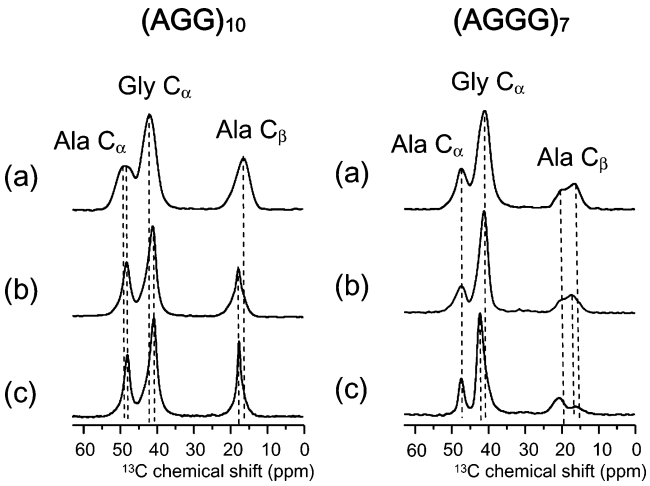

Figure 3. ^{13}C CP/MAS NMR spectra of Ala-Gly repeated model peptides, $(AGG)_{10}$ and $(AGGG)_7$ as Figure 2.

$(AGGG)_7$ was synthesized and the ^{13}C CP/MAS NMR spectra were observed after three kinds of treatments (Figure 3, right). Lotz and Keith[34,35] reported that poly(AGGG) took essentially the same structure as poly(Gly) II ($\varphi = -70°$ and $\psi = 140°$) when the sample was prepared by dialyzing 1% solutions of

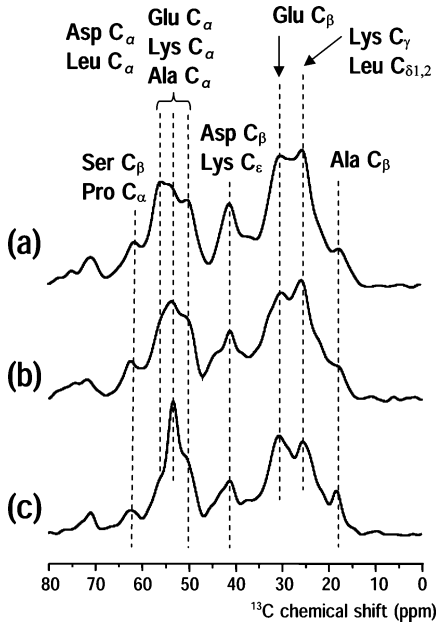

Figure 4. ^{13}C CP/MAS NMR spectra of D_{9k}-loop (D_{9k}L) peptide as Figure 2. The peak assignments are included.

polypeptide against 60% aqueous LiBr (agitation tends to precipitate the β-modification). We prepared a higher concentration of the peptide samples in 9 M LiBr and dialyzed it against water directly. Therefore, the main structure of $(AGGG)_7$ after our LiBr treatment is expected to be a mixture of poly(Gly) II ($\varphi = -70°$ and $\psi = 140°$) and β-sheet structure. The broad doublet peak (17.8 and 21.1 ppm) (Figure 3b) of Ala C_β supports this speculation. However, the peak at 17.8 ppm is still broad even when overlapped by the β-sheet peak, indicating a large distribution of the torsion angles and that the structure reflecting 17.8 ppm peak is a distorted 3_1-helix. A similar spectral pattern was also observed for the peptide after TFA treatment, but the main peak of Ala C_β shifted slightly to a higher field (16.5 ppm), indicating a mixture of random coil and β-sheet. After FA treatment, the ^{13}C CP/MAS NMR pattern of the peptide changed significantly. Judging from the spectral pattern, the main structure is β-sheet together with significant amount of random coil structure. This is also supported by the sharper spectral pattern in TFA compared with either LiBr or FA treatments.

Secondary Structures of the Four Peptides Containing the Ca^{2+} Binding Sequence from Calbindin D_{9k}. Figure 4 shows ^{13}C CP/MAS NMR spectra of only D_{9k}L (GAAKEGDPNQL-SKEEG) without the Ala-Gly repeating sequence. The effects of TFA, LiBr, and FA treatments are shown. The peak assignments are indicated by arrows. A more detailed assignment is difficult because of the severe peak overlap, especially in the C_α resonance regions. The spectral pattern was almost the same after TFA and LiBr treatments. However, the spectrum after FA treatment was markedly different, especially in the C_α resonance regions. No further analysis was attempted.

Figure 5 shows the ^{13}C CP/MAS NMR spectra of $(A)_{12}$-D_{9k}L and $(AG)_6$-D_{9k}L, after TFA, LiBr, and FA treatments. As mentioned above, the Ala C_β region (approximately 20 ppm) contains a great deal of structural information. Accordingly, difference spectra (green lines) were prepared for this part of spectrum to give information from only the repeating poly(Ala) or poly(Ala-Gly) domains by subtracting the contribution of D_{9k}L without these domains (red lines) from the spectra obtained for peptides containing both D_{9k}L and these domains (blue lines). The ^{13}C chemical shifts of $(A)_{12}$-D_{9k}L and $(AG)_6$-D_{9k}L are listed in Table 2.

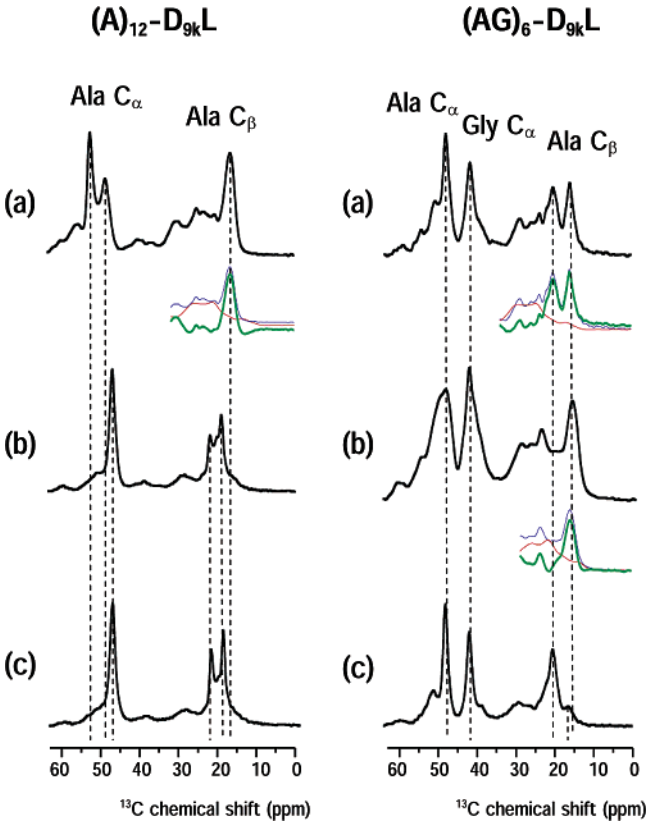

Figure 5. ^{13}C CP/MAS NMR spectra of $(A)_{12}$-D_{9k}L and $(AG)_6$-D_{9k}L peptides as Figure 2. The amino acid sequences of these peptides are listed in Table 1. Difference spectra (thick green spectra) of silk-like peptides containing D_{9k}L sequences were prepared by subtracting the spectra from the D_{9k}L sequence without the flanking peptides (red) from the original spectra (blue).

For $(A)_{12}D_{9k}$L treated with TFA, the Ala C_α peak was observed at 52.6 ppm and Ala C_β at 15.9 ppm. The latter chemical shift did not change after subtracting the contribution from the D_{9k}L domain, giving only a single Ala C_β peak in the difference spectrum. Thus, the poly(Ala) region in the peptide $(A)_{12}$-D_{9k}L takes exclusively an α-helix. This indicates that the presence of the D_{9k}L domain has no influence on the inherent structure of poly(Ala) after TFA treatment. Although the peaks from Ala C_α and Ala C_β of the peptide $(A)_{12}$-D_{9k}L overlap with the C_α and C_β peaks of the D_{9k}L domain, the chemical shifts of C_α, C_β, and C═O of Ala residues show that the conformation of poly(Ala) was β-sheet after LiBr and FA treatments. These results show that the poly(Ala) region in $(A)_{12}$-D_{9k}L after TFA treatment formed the α-helix and the conformation changed from α-helix to β-sheet after LiBr and FA treatments. Thus, the presence of D_{9k}L domain in $(A)_{12}$-D_{9k}L does not affect the α-helix to β-sheet conformational transition in the poly(Ala) domain. Two sharp peaks were observed in the Ala C_β region for $(A)_{12}$-D_{9k}L after FA treatment although both can be assigned to β-sheet structure. This means that there were two clearly different β-sheet structures. Deeper analysis of these requires further work.

In contrast to $(A)_{12}$-D_{9k}L, there are significant differences between the spectra of $(AG)_6$-D_{9k}L and those of $(AG)_{15}$ without D_{9k}L. Two Ala C_β peaks were observed at 20.8 and 16.1 ppm after TFA treatment of $(AG)_6$-D_{9k}L. The difference spectrum after subtraction of the contribution from D_{9k}L shows that the relative peak intensity is not changed compared with the original unsubtracted spectrum. However the fraction of silk II was significantly increased in the case, $(AG)_6$-D_{9k}L. In contrast, LiBr

Table 3. ^{13}C CP/MAS NMR Chemical Shifts (in ppm from TMS) of ^{13}C-labeled Carbons of Amino Acid Residues in $(A)_{12}$-D_{9k} Peptides after TFA, LiBr, and FA Treatments

	TFA treatment			LiBr treatment			FA treatment		
carbon in amino acids	chemical shifts (ppm)	Δ ppm[a]	conformation	chemical shifts (ppm)	Δ ppm[a]	conformation	chemical shifts (ppm)	Δ ppm[a]	conformation
Ala^7 C=O	176.0	4.7	α-helix	171.5	0.2	β-sheet	171.8	0.5	β-sheet
Ala^{13} C_α	52.4	2.4	α-helix	48.6	−1.8	β-sheet	48.9	−1.1	β-sheet
Ala^{14} C_β	15.7	−0.9	α-helix	16.4	−0.2	random coil and β-sheet	16.9	0.3	random coil and β-sheet
				19.8	3.2		20.1	3.5	
				22.6	6.0		23	6.4	
Gly^{17} C_α	42.6	−0.1	random coil	42.5	−0.2	β-sheet	42.6	−0.1	β-sheet

[a] Δ ppm indicates the difference in the chemical shift (in ppm) before and after each treatment.

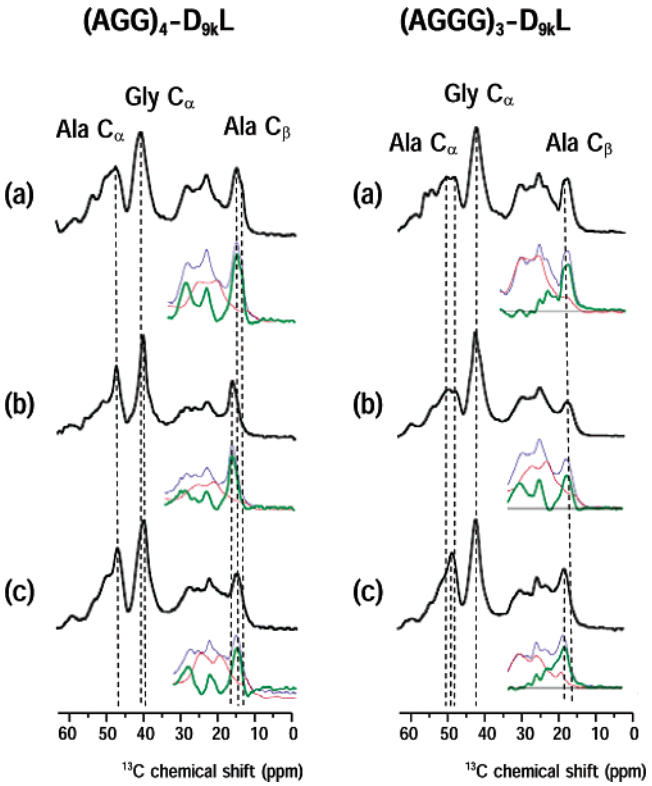

Figure 6. ^{13}C CP/MAS NMR spectra of $(AGG)_4$-$D_{9k}L$ and $(AGGG)_3$-$D_{9k}L$ peptides as Figure 5.

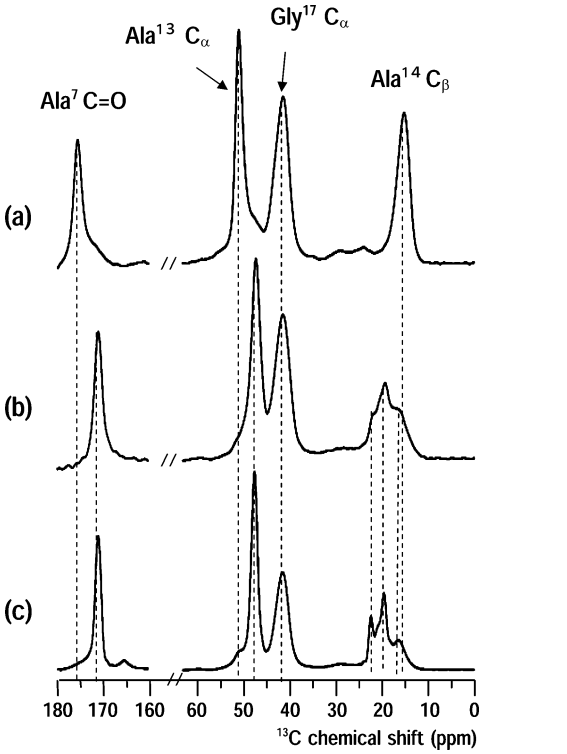

Figure 7. ^{13}C CP/MAS NMR spectra of ^{13}C-labeled $(A)_{12}$-D_{9k} peptide, AAAAAA[1-^{13}C]AAAAA A[2-^{13}C]A[3-^{13}C]AKE[2-^{13}C]GDPNQLSKEE-AAAAAAAAAAAA as Figure 5.

treatment of $(AG)_6$-$D_{9k}L$ gave an Ala C_α peak at 50.0 ppm, Ala C_β peak at 16.4 ppm, and Gly C_α peak at 42.8 ppm (Figure 5, right). The difference spectrum after subtraction of the contribution from $D_{9k}L$ gave a single broad Ala C_β peak. Thus, comparing the effect of LiBr treatment on the peptides $(AG)_{15}$ and $(AG)_6$-$D_{9k}L$ showed that the $D_{9k}L$ domain changes the conformation of the poly(AG) from silk I to random coil conformation. $(AG)_6$-$D_{9k}L$ after FA treatment showed the Ala C_α peak at 48.9 ppm and the Ala C_β peak at 20.9 ppm as main peaks. In addition, shoulder peaks at 17.9 and 22.3 ppm for Ala C_β were also observed. This indicates that the peptide after FA treatment takes the silk II structure.

As shown in Figure 6 (left), the peptide, $(AGG)_4$-$D_{9k}L$, took random coil structure after TFA treatment, which is similar to the structure of $(AGG)_{10}$ without $D_{9k}L$ under these conditions. The absence of β-sheet structure is clear from the difference spectrum. The chemical shift 17.1 ppm of Ala C_β of the difference spectrum for $(AGG)_4$-$D_{9k}L$ showed that poly(AGG) domain adopted a distorted 3_1-helix after LiBr treatment. FA treatment markedly changed the difference spectrum. The peak shifts to 16.4 ppm and becomes broader, which is quite different from the corresponding spectrum of $(AGG)_{15}$ without $D_{9k}L$ under the same condition (Figure 5, left). This indicates that, in the case of FA treatment, the $D_{9k}L$ domain in $(AGG)_4$-$D_{9k}L$ is able to convert the 3_1-helix seen in the peptide $(AGG)_{15}$ to random coil.

The conformation of $(AGGG)_3$-$D_{9k}L$ (Figure 6, right) appeared to be random coil after both TFA and LiBr treatments as the Ala C_β peaks were slightly shifted to the random coil position and were sharper compared with the corresponding spectra of $(AGGG)_7$ without $D_{9k}L$. The difference spectra also support this interpretation. Only a small amount of β-sheet structure was detected after TFA treatment, whereas this component appeared to be entirely absent after LiBr treatment. After FA treatments, the conformation also appeared to be mainly random coil in contrast to the peptide $(AGGG)_7$ without $D_{9k}L$ which was predominantly β-sheet under the same conditions. The difference spectrum for $(AGGG)_3$-$D_{9k}L$ indicates the presence of a small amount of β-sheet after FA treatment, but the amounts decrease considerably. Again, the presence of the $D_{9k}L$ domain appeared to alter the conformation of the added silk-like domain after FA treatment.

In summary, the poly(Ala) domains retain the ability to undergo a conformational transition from α-helical to β-sheet in $(A)_{12}$-$D_{9k}L$ despite the presence of the $D_{9k}L$ domain at the center of the peptide molecules, but the presence of this domain

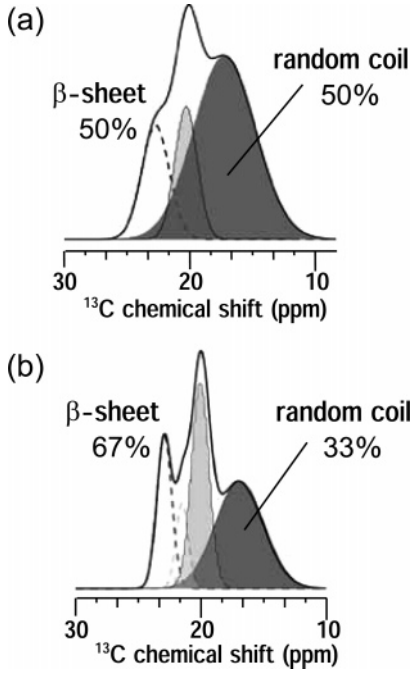

Figure 8. Deconvoluted Ala C_β peaks in the ^{13}C CP/MAS NMR spectra of ^{13}C-labeled A_{12}-D_{9k} after LiBr treatment (a) and FA treatment (b).

in the other model peptides synthesized has a marked effect on the conformation of the added silk-like domains.

Secondary Structure of Ca^{2+} Binding Sequence, $D_{9k}L$, in ^{13}C-Labeled $(A)_{12}$-$D_{9k}L$ after TFA, LiBr, and FA Treatments. Having investigated the effect of our standard treatments on the poly(Ala) domains in $(A)_{12}$-$D_{9k}L$ (see above), we also investigated their effect on the $D_{9k}L$ sequence in the center of the same peptide. For this, we synthesized the ^{13}C labeled peptide, AAAAAA[1-^{13}C]AAAAAA[2-^{13}C]A[3-^{13}C]AKE[2-^{13}C]GPNQLSKEEAAAAAAAAAAAA, (see Table 1). Figure 7 shows ^{13}C CP/MAS NMR spectra of the ^{13}C-labeled $(A)_{12}$-$D_{9k}L$ after TFA, LiBr, and FA treatments. The ^{13}C chemical shifts of this peptide are listed in Table 3. In the ^{13}C CP/MAS NMR spectra, the C═O peaks of Ala[7] shifts after TFA (176.0 ppm), LiBr (171.5 ppm), and FA (171.8 ppm) treatments indicated an α-helical conformation after TFA and *β*-sheet after both LiBr and FA treatments. However, the structure of Gly[17] was random coil after all three treatments. The local structures of Ala[13] and Ala[14] were similar to that of Ala[7], Ala[13], and Ala,[14] taking α-helical structure after TFA treatment and *β*-sheet after both LiBr and FA treatments judging from the C_α and C_β chemical shifts. However, shoulder peaks were observed at around 16∼17 ppm in the Ala[14] peaks after both LiBr and FA treatments, indicating the presence of small fractions of an additional conformation. To perform detailed conformational

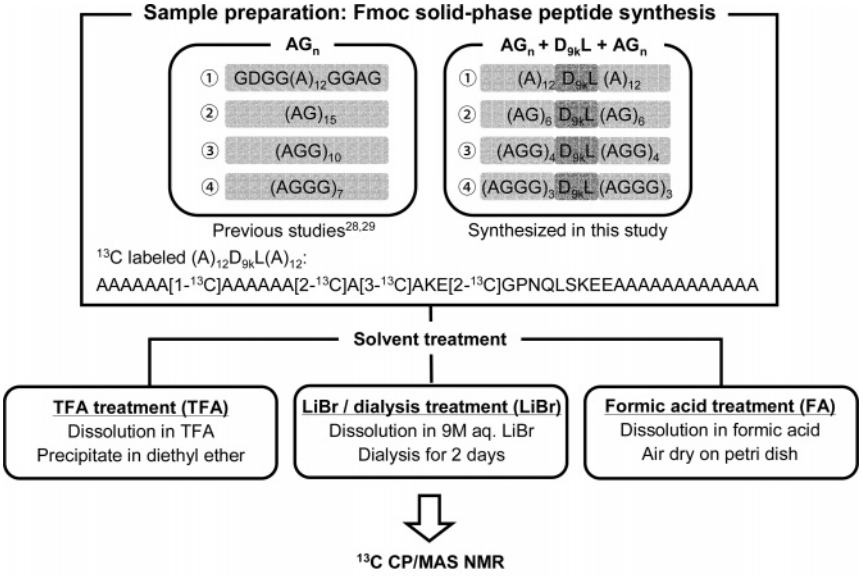

Peptides	Conformation after treatment		
	TFA	LiBr	FA
GDGG(A)$_{12}$GGAG	*α*-helix	*β*-sheet	*β*-sheet
(A)$_{12}$-D$_{9k}$L-(A)$_{12}$	*α*-helix	*β*-sheet	*β*-sheet
(AG)$_{15}$	random coil silk II	silk I	silk II
(AG)$_6$-D$_{9k}$L-(AG)$_6$	random coil silk II	random coil	silk II
(AGG)$_{10}$	random coil	3$_1$-helix	3$_1$-helix
(AGG)$_4$-D$_{9k}$L-(AGG)$_4$	random coil	3$_1$-helix	random coil
(AGGG)$_7$	random coil *β*-sheet	3$_1$-helix *β*-sheet	random coil *β*-sheet
(AGGG)$_3$-D$_{9k}$L-(AGGG)$_3$	random coil	random coil	random coil *β*-sheet

Figure 9. Flowchart illustrating the experimental procedures and the corresponding results.

analysis, the C_β peak of Ala^{14} residue after LiBr and FA treatments were deconvoluted (Figure 8). This deconvolution gave 50% random coil and 50% β-sheet structure after LiBr treatment, and 33% random coil and 67% β-sheet structure after FA treatment. Thus after LiBr and FA treatments, the random coil portion of Ala^{14} in the D_{9k} domain was greater than that in the $(Ala)_{12}$ domains in the model peptide. These results suggest that the conformation of the calcium-binding loop region is mainly in random coil state, and is not affected by the presence of $(Ala)_{12}$ in the β-sheet conformation.

In summary, our observations suggested that the calcium-binding loop maintained an appropriate conformation to retain its function regardless of the presence of the different flanking silk-derived repetitive sequences used in this study. The experimental procedures and the corresponding results are summarized in Figure 9.

Conclusions

In the present paper, we described the synthesis of several model peptides containing silk-like sequences flanking a central calcium-binding motif derived from calbindin, the D_{9k}-loop ($D_{9k}L$). In the four synthesized peptides containing $D_{9k}L$, the flanking silk-like domains showed different secondary structures after standard treatments known to modify α-helix, β-sheet, and 3_1-helix contents in other silk proteins and silk-like peptides. We observed that the amino acid residues in $D_{9k}L$ had a predominantly random coil structure and that the random coil fraction increased after the treatments used. In addition, we have shown that poly(Ala) domains retain their ability to undergo a conformation transition from α-helical to β-sheet when flanking the $D_{9k}L$ domain.

These findings may provide a first step toward the development of novel protein materials combining biocompatibility, good mechanical properties, and calcium-binding capability with potential uses as implantable materials. In addition, the inclusion of EF hand motifs in larger synthetic silk-like peptides may facilitate processing into useful materials by emulating the calcium binding sites thought to be important for the storage and natural spinning of lepidopteran fibroins.

Acknowledgment. T.A. acknowledges supports from the Insect Technology Project, Japan and Agriculture Biotechnology Project, Japan.

References and Notes

(1) Gosline, M. J.; Guerette, A. P.; Ortlepp, S. C.; Savage, N. K. The mechanical design of spider silks: from fibroin sequence to mechanical function. *J. Exp. Biol.* **1999**, *202*, 3295−3303.
(2) Craig, C. L. Evolution of arthropod silks. *Annu. Rev. Entomol.* **1997**, *42*, 231−267.
(3) Suzuki, Y.; Brown, D. D. Isolation and Identification of the messenger RNA for silk fibroin from *Bombyx mori*. *J. Mol. Biol.* **1972**, *63*, 409−429.
(4) Zhou, C. Z.; Confalonieri, F.; Medina, N.; Zivanovic, Y.; Esnault, C.; Yang, T.; Jacquet, M.; Janin, J.; Duguet, M.; Perasso, R. Fine organization of *Bombyx mori* fibroin heavy chain gene. *Nucleic Acids Res.* **2000**, *28*, 2413−2419.
(5) Sezutsu, H.; Yukuhiro, K. Dynamic rearrangement within the *Antheraea pernyi* silk fibroin gene is associated with four types of repetitive units. *J. Mol. Evol.* **2000**, *51*, 329−338.
(6) Hwang, J. S.; Lee, J. S.; Goo, T. W.; Yun, E. Y.; Lee, K. S.; Kim, Y. S.; Jin, B. R.; Lee, S. M.; Kim, K. Y.; Kang, S. W.; Suh, D. S. Cloning of the fibroin gene from the oak silkworm − *Antheraea* yamamai and its complete sequence. *Biotechnol. Lett.* **2001**, *23*, 1321−1326.
(7) Hinman, M. B.; Lewis, R. V. Isolation of a clone encoding a 2nd dragline silk fibroin − *Nephila clavipes* dragline silk is a 2-protein fiber. *J. Biol. Chem.* **1992**, *267*, 19320−19324.
(8) Kong, X. D.; Cui, F. Z.; Wang, X. M.; Zhang, M.; Zhang, W. Silk fibroin regulated mineralization of hydroxyapatite nanocrystals. *J. Cryst. Growth* **2004**, *270*, 197−202.
(9) Sofia, S.; McCarthy, M. B.; Gronowicz, G.; Kaplan, D. L. Functionalized silk-based biomaterials for bone formation. *J. Biomed. Mater. Res.* **2001**, *54*, 139−148.
(10) Hossain, K. S.; Nemoto, N.; Magoshi, J. Dynamic and static light scattering of dilute aqueous solutions of silk fibroin collected from *Bombyx mori* silkworms. *Langmuir* **1999**, *15*, 4114−4119.
(11) Hossain, K. S.; Nemoto, N.; Magoshi, J. Rheological study on aqueous solutions of silk fibroin extracted from the middle division of *Bombyx mori* silkworm. *Nihon Reoroji Gakkaishi* **1999**, *27*, 129−130.
(12) Terry, A. E.; Knight, D. P.; Porter, D.; Vollrath, F. PH induced changes in the rheology of silk fibroin solution from the middle division of *Bombyx mori* silkworm. *Biomacromolecules* **2004**, *5*, 768−772.
(13) Ping, Z.; Xun, X.; Knight, D. P.; Zong, X. H.; Feng, D.; Yao, W. H. Effects of pH and calcium ions on the conformational transitions in silk fibroin using 2D Raman correlation spectroscopy and C-13 solid-state NMR. *Biochemistry* **2004**, *43*, 11302−11311.
(14) Bini, E.; Knight, D. P.; Kaplan, D. L. Mapping domain structures in silks from insects and spiders related to protein assembly. *J. Mol. Biol.* **2004**, *335*, 27−40.
(15) Huang, X.; Miller, W. A time-efficient, linear-space local similarity algorithm. *Adv. Appl. Math.* **1991**, *12*, 337−357.
(16) Knight, D. P. **2005** unpublished result.
(17) Drescher, D.; De Luca, H. F. Vitamin D-Stimulated Calcium Binding Protein from Rat Intestinal Mucosa − Purification and Some Properties. *Biochemistry* **1971**, *10*, 2302−2307.
(18) Fullmer, C. S.; Wasserman, R. H. The amino acid sequence of bovine intestinal calcium-binding protein. *J. Biol. Chem.* **1981**, *256*, 5669−5674.
(19) Christakos, S.; Gabrielides, C.; Rhoten, W. B. Vitamin D-dependent calcium binding proteins: Chemistry, distribution, functional considerations, and molecular biology. *Endoc. Rev.* **1989**, *10*, 3−26.
(20) Kretsinger, R. H.; Nockolds, C. E. Carp Muscle Calcium-binding Protein. II. Structure determination and general description. *J. Biol. Chem.* **1973**, *248*, 3313−3326.
(21) Szebenyi, D. M.; Moffat, K. The refined structure of vitamin D-dependent calcium-binding protein from bovine intestine. *J. Biol. Chem.* **1986**, *261*, 8761−8776.
(22) Kordel, J.; Skelton, N. J.; Akke, M.; Chazin, W. J. High-resolution solution structure of calcium-loaded calbindin D_{9k}. *J. Mol. Biol.* **1993**, *231*, 711−734.
(23) Skelton, N. J.; Kordel J.; Chazin W. J. Determination of the solution structure of apo calbindin D_{9k} by NMR spectroscopy. *J. Mol. Biol.* **1995**, *249*, 441−462.
(24) Nakazawa, Y.; Asakura, T. Structure determination of a peptide model of the repeated helical domain in *Samia cynthia ricini* silk fibroin before spinning by a combination of advanced solid-state NMR methods. *J. Am. Chem. Soc.* **2003**, *125*, 7230−7237.
(25) Asakura, T.; Ashida, J.; Yamane, T.; Kameda, T.; Nakazawa, Y.; Ohgo, K.; Komatsu, K. A repeated β-turn structure in poly(Ala-Gly) as a model for silk I of *Bombyx mori* silk fibroin studied with two-dimensional spin-diffusion NMR under off magic angle spinning and retational echo double resonance. *J. Mol. Biol.* **2001**, *306*, 291−305.
(26) Asakura, T.; Yao, J. M. ^{13}C CP/MAS NMR study on structural heterogeneity in *Bombyx mori* silk fiber and their generation by stretching. *Protein Sci.* **2002**, *11*, 2706−2713.
(27) Asakura, T.; Yang, M.; Kawase, T. Structure of Characteristic Sequences in *Nephila clavipes* Dragline Silk (MaSp1) Studied with ^{13}C Solid State NMR. *Polym. J.* **2004**, *36*, 999−1003.
(28) Ashida, J.; Ohgo, K.; Komatsu, K.; Kubota, A.; Asakura, T. Determination of the torsion angles of alanine and glycine residues of model compounds of spider silk $(AGG)_{10}$ using solid-state NMR methods. *J. Biomol. NMR* **2003**, *25*, 91−103.
(29) Yang, M. Y.; Asakura, T. Design, expression and solid-state NMR characterization of silk-like materials constructed from sequence of spider silk, *Samia cynthia ricini* and *Bombyx mori* silk fibroins. *J. Biochem.* **2005**, *137*, 721−729.
(30) Wildman, K. A. H.; Lee, D. K.; Ramamoorthy, A. Determination of α-helix and β-sheet stability in the solid state: A solid-state investigation of poly(L-alanine). *Biopolymers* **2002**, *64*, 246−254.
(31) Nakazawa, Y.; Bamba, M.; Nishio, S.; Asakura, T. Tightly winding structure of sequential model peptide for repeated helical region in Samia cynthia ricini silk fibroin studied with solid-state NMR. *Protein Sci.* **2003**, *12*, 666−671.

(32) Asakura, T.; Ohgo, K.; Komatsu, K.; Kanenari, N.; Okuyama, K. Refinement of repeated β-turn structure for silk I conformation of *Bombyx mori* silk fibroin using ^{13}C solid-state NMR and X-ray diffraction methods. *Macromolecules* **2005**, *38*, 7397−7403.
(33) Asakura, T.; Yao, J. M.; Yamane, T.; Umemura, K.; Ulrich, K. S. Heterogeneous structure of silk fibers from *Bombyx mori* resolved by ^{13}C solid-state NMR spectroscopy. *J. Am. Chem. Soc.* **2002**, *124*, 8794−8795.
(34) Lotz, B.; Keith, H. D. The crystal structures of poly(L-Ala-Gly-Gly-Gly)II and poly(L-Ala-Gly-Gly)II. *J. Mol. Biol.* **1971**, *61*, 195−200.
(35) Wildman, K. A. H.; Wilson, E. E.; Lee, D. K.; Ramamoorthy, A. Determination of the conformation and stability of simple homopolypeptides using solid-state NMR. *Solid State Nucl. Magn. Reson.* **2003**, *24*, 94−109.

BM050863Q